The Journal of Engineering

The 14th IET International Conference on AC and DC Power Transmission (ACDC 2018)

IET Journals
The Institution of Engineering and Technology

Unbalanced power flow algorithm for AC&DC hybrid distribution network with diverse-controlled VSC-MTDC converts

eISSN 2051-3305
Received on 4th September 2018
Accepted on 19th September 2018
E-First on 17th December 2018
doi: 10.1049/joe.2018.8888
www.ietdl.org

Dehua Chen[1], Xingquan Ji[1] ✉, Yongjin Yu[1], Xingzhen Bai[1], Jinxiao Liu[2]

[1]College of Electrical Engineering and Automation, Shandong University of Science and Technology, Qingdao, People's Republic of China
[2]Qihe Power Supply Company of State Grid Shandong Electric Power Company, Dezhou, People's Republic of China
✉ *E-mail: eesdust@qq.com*

Abstract: The paper aims to propose an algorithm to calculate the power flow of an AC&DC hybrid distribution system. AC&DC distribution networks have recently attracted increasing attention, for the distributed generations (DGs) and DC loads can be integrated in DC networks in more simple and flexible ways than AC networks. Many efforts have been made to deal with the power flow problem of hybrid networks, however, the DC-side power flow's effect on three-phase unbalanced AC side and the influence to entire distribution system which DG directly connected in the DC side are both not considered. Therefore, this paper discusses the grid architecture with multiple AC&DC feeders. Then, models of VSC-MTDC, DC/DC converters, DGs, and other elements are formulated for power flow calculation. Furthermore, power flow equations of DC distribution and VSC converters are deduced in detail. As for converters under different control strategies and diverse forms of linking combinations between AC&DC grids, calculating approaches are considered to be of partial differences. Considering these distinct cases, a specific and improved sequential method is employed to compute distribution network's power flow. Simulation results on a modified IEEE 13 Node Test Feeder demonstrate the rapidity, accuracy, and easy-convergence of the algorithm.

1 Introduction

With the development of power electronic technology and DC relay protection devices, as well as the increasing popularity of multi-terminal converters and high-power DC devices, the development of AC&DC distribution network is becoming much more significant. Compared to the AC distribution networks, DC distribution networks obviously possess more advantages [1]. It is apparent that while AC grids are three-phase four-wire systems, only two wires are required for DC power transmission, and the cost for installing DC networks are less than that for AC; without any AC/DC converters, the DC electrical equipment can be directly connected to the DC networks, which will help reduce losses and save costs; the power transmission by DC distribution system in 'single-phase' manner, no three phase and angle limitation or rather three-phase unbalanced problem, helps to improve the quality of electricity; the DC bus only has the voltage magnitude and the active power so that the distributed generation needs merely the DC/DC conversion or the AC/DC conversion to instantly connect to the network without overmuch adjustment; due to the development of bi-directional DC/DC converting technology, certain electrical devices, such as electric vehicles, on the user side can be switched from a charged state to a discharged state when required by the grid with energy feeding back to and support the grid. Owing to these advantages of DC distribution network, it can be expected that the AC distribution network will be developed into a hybrid AC&DC network in the near future [2].

A lot of work has been done on the research of hybrid AC&DC grids. In [3], the losses of converters are ignored and the VSC operating set point is specified at the converter bus instead of at the point of common coupling bus. In [4], different control strategies of VSC and Gauss–Seidel methods are considered. In [5], a detailed VSC station model with filter and converter losses is presented. DC slack control was studied in [4, 5], while voltage droop control was considered in [3, 6]. These literatures mainly focus on the equivalent treatment of converter interface and the iterative method of AC&DC mixed power flow, and do not describe the topology of AC&DC power distribution network, or do either not consider the three-phase unbalanced problem in distribution network. The DC-side distributed generations and energy storage equipment are also not considered.

This paper describes the topology of DC distribution network considering different application scenarios. Then, the power flow calculation model of VSC converters with diverse control method is analysed. Moreover, DC models about the electric energy generation, storage and usage including DG, storage battery, DC load and so on have been established. According to the various control strategies of VSC-MTDC and the topology of DC distribution network, the iterative calculation method of hybrid AC&DC power flow is minutely illustrated. Finally, a case of IEEE 13 Node Test Feeder is remoulded with DC grid added in it in order to stimulate the algorithm.

2 Model

2.1 Three-phase AC model

Taking into account the three-phase unbalanced condition, three-phase modelling method is adopted in the calculation of power flow. The detailed AC models which can be found in many references [7, 8] are not listed here.

2.2 AC&DC distribution network architecture

There are four common architectures presented here, which are shown in Fig. 1.

2.2.1 Radial configuration: As is shown in Fig. 1*a*, radical structure is the most basic topology. Each load can only get electricity from one path, meanwhile, user-side distributed power and energy storage devices can achieve instantly integration in DC grids. Not only the structure, operation, and control are simple, but compatibility with AC systems is favourable.

2.2.2 Hand-in-hand configuration: Fig. 1*b* exhibits the hand-in-hand structure. The DC bus receives power from two power-supply terminals and delivers it to the loads. Simultaneously, distributed power transmits energy through two directions on grid buses. When one side of power supply fails, the load can be switched to the other side through the tie switch, which will not result in outage in entire area and increase the reliability of the power supply.

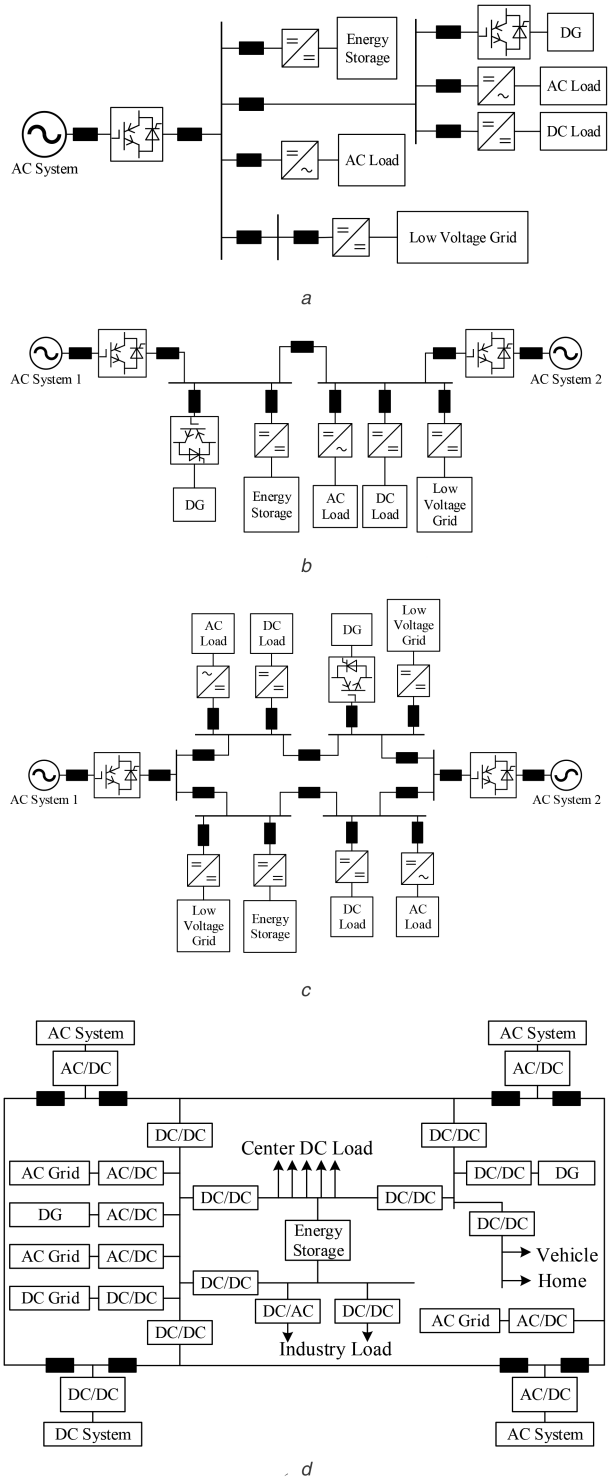

Fig. 1 *Architectures of DC distribution network*
(a) Radial, ***(b)*** Hand in hand, ***(c)*** Circle, ***(d)*** Mesh

2.2.3 Ring network: Circle structure, shown in Fig. 1*c*, has higher power supply reliability. When any bus in the loop faults, the protection devices act quickly to locate and isolate the faults. The remaining distribution sections operate properly in accordance with the hand-in-hand structure and without cutting off loads. Compared with the latter structure, bus-tie switch is eliminated.

2.2.4 Meshed network: In Fig. 1*d*, combined by the above three structures freely, the mesh structure represents the future development trend of hybrid AC&DC distribution network, which contains multiple voltage levels and facilitates reliability and flexibility of power supply.

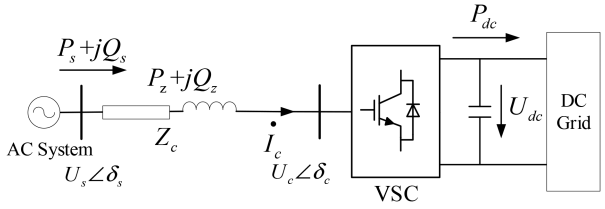

Fig. 2 *VSC scheme*

2.3 VSC steady-state model

In order to derive the power flow model equations of the VSC converter, we assume that: (i) All converters are three phase symmetrical; (ii) The converts' DC outlet voltage and current are ideal flat voltage and current.

In Fig. 2, P_s and Q_s are, respectively, the active power and reactive power of the AC bus which is connected with a VSC converter. $U_s\angle\delta_s$ is the voltage magnitude and angle of the AC bus. $U_c\angle\delta_c$ is the voltage magnitude and angle of the AC outlet of the converter. $Z_c = R_c + jX_c$ is the equivalent impedance representing the commutation loss, where R_c is the total equivalent resistances of the commutating phase reactors and converter transformers, and X_c is the equivalent reactance of the reactors. Finally, $P_{\rm dc}$ is the active power at DC side of converter, while $U_{\rm dc}$ is the voltage on converter's DC bus.

The key to modelling the converter is confirming its outlet modulation voltage U_c. Symmetrical component method is applied to obtain U_c. Let $\dot{U}_{\rm cj}$ ($j = 0, 1, 2$) be its sequence component expression. Due to the symmetrical structure of the converter, it can be considered that the output modulation voltage only contains positive sequence component $\dot{U}_{s0}$. let $\dot{U}_{\rm sj}$ ($j = 0, 1, 2$) be the voltage sequence component of the AC-side bus. First, as is shown in (1), the sequence components about voltage vector at AC side of converter is given by

$$\begin{bmatrix}\dot{U}_{s0}\\ \dot{U}_{s1}\\ \dot{U}_{s2}\end{bmatrix} = \frac{1}{3}\begin{bmatrix}1 & 1 & 1\\ 1 & \alpha & \alpha^2\\ 1 & \alpha^2 & \alpha\end{bmatrix}\begin{bmatrix}\dot{U}_{\rm sa}\\ \dot{U}_{\rm sb}\\ \dot{U}_{\rm sc}\end{bmatrix} \tag{1}$$

where $\dot{U}_{\rm sa}$, $\dot{U}_{\rm sb}$, $\dot{U}_{\rm sc}$ represent three-phase AC voltage phasor.

The positive sequence voltage drop on the reactor's internal reactance can be obtained by

$$\begin{cases}\Delta U = \dfrac{Q_s X_c + P_s R_c}{|\dot{U}_{s1}|}\\ \delta U = \dfrac{P_s X_c - Q_s R_c}{|\dot{U}_{s1}|}\end{cases} \tag{2}$$

where ΔU and δU are, respectively, horizontal and vertical components of the voltage drop on the reactor inside the converter, so that outlet modulation voltage's positive sequence component is

$$\dot{U}_{c1} = \dot{U}_{s1} + \Delta U + j\delta U \tag{3}$$

Then, according to the positive, negative, and zero sequential values of the converter output modulation voltage (negative and zero sequences of components are both zero), the three-phase voltage values can be obtained by

$$\begin{bmatrix}\dot{U}_{\rm ca}\\ \dot{U}_{\rm cb}\\ \dot{U}_{\rm cc}\end{bmatrix} = \begin{bmatrix}1 & 1 & 1\\ 1 & \alpha^2 & \alpha\\ 1 & \alpha & \alpha^2\end{bmatrix}\begin{bmatrix}\dot{U}_{c0}\\ \dot{U}_{c1}\\ \dot{U}_{c2}\end{bmatrix} \tag{4}$$

where $\dot{U}_{\rm ca}$, $\dot{U}_{\rm cb}$, $\dot{U}_{\rm cc}$ is the converter outlet modulation voltage vector.

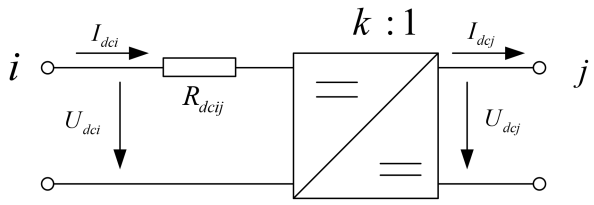

Fig. 3 *DC/DC converter scheme*

Table 1 Conversion steps of grid connection for DGs

Device	Paralleling in AC grid	Paralleling in DC grid
photovoltaic	DC/DC, DC/AC	DC/DC
wind	AC/DC, DC/AC	AC/DC
fuel	DC/DC, DC/AC	DC/DC
storage	DC/DC, DC/AC	DC/DC

After confirming the converter's outlet modulation voltage U_c, the three-phase injection current can be obtained as shown in (5).

$$\dot{I}_{\mathrm{ci}} = \frac{\dot{U}_{\mathrm{ci}} - \dot{U}_{\mathrm{si}}}{R_c + jX_c}. \quad i = a, b, c \tag{5}$$

In addition, the converter must also satisfy the voltage and power constraints:

$$\dot{U}_c = \frac{\mu M}{\sqrt{2}} U_{\mathrm{dc}} \tag{6}$$

$$P_s = P_z + P_{\mathrm{loss}} + P_{\mathrm{dc}} \tag{7}$$

where μ is the DC voltage utilisation rate, when adopting sine pulse width modulation, the number is $\sqrt{3}/2$, and likewise employing space vector modulation is 1. M is the modulation coefficient and $0 \le M \le 1$. P_z represents the active power loss of the resistor R_c and P_{loss} is the power loss of the converter, P_z and P_{loss} can be calculated by

$$P_z = \sum_{i=a}^{c} I_{\mathrm{ci}}^2 R_{\mathrm{ci}}. \quad i = a, b, c \tag{8}$$

$$P_{\mathrm{loss}} = \frac{1}{3} \sum_{i=a}^{c} (a + bI_{\mathrm{ci}} + cI_{\mathrm{ci}}^2). \quad i = a, b, c \tag{9}$$

In (9), the coefficients a, b, and c are constants: a simulates the inherent active power loss that is irrelevant to the current; b simulates active power loss that is proportional to current; c simulates the active loss that is proportional to the square of current. The coefficients a, b, and c can be acquired and recorded through engineering operations, which specifically refers to [9, 10].

The active power of the VSC converter injected into the DC side is as follows

$$P_{\mathrm{dc}} = U_{\mathrm{dc}} I_{\mathrm{dc}} \tag{10}$$

Finally, using (5)–(10), the current injected into AC and DC systems by the converter can be obtained, and the power flow iterative calculation can be completed. Moreover, the power flow calculation model of one VSC converter station is formed by (1)–(10).

2.4 DC component model

2.4.1 DC line model: The DC networks can be represented by a resistive network. Each branch has resistance R_{dcij} that can compose branch resistance matrix:

$$\boldsymbol{Y}_{\mathrm{dcl}} = \begin{bmatrix} \boldsymbol{Y}_D & -\boldsymbol{Y}_D \\ -\boldsymbol{Y}_D & \boldsymbol{Y}_D \end{bmatrix} \tag{11}$$

with $Y_{\mathrm{Dij}} = 1/R_{\mathrm{dcij}}$. Therefore, the DC node admittance matrix results from

$$\boldsymbol{Y}_{\mathrm{dc}} = \boldsymbol{C}_m \boldsymbol{Y}_{\mathrm{dcl}} \boldsymbol{C}_m^T \tag{12}$$

where $\boldsymbol{C}_m$ is an incidence matrix, with the element $\boldsymbol{C}_{\mathrm{mij}} = 1$ if the branch i and the bus j are incident and 0 otherwise.

2.4.2 DC/DC converter model: In multiple voltage-level DC distribution network, the adjacent buses of different voltage levels need to be connected by DC/DC converters as shown in Fig. 3.

In Fig. 3, U_{dcx} and I_{dcx} indicate the DC buses' voltages and currents, respectively. In the interim, the resistance R_{dcij} is equivalent to converter's internal loss, and the factor k is the converter ratio, which can be used to calculate branch resistance matrix Y_{Dij} by

$$Y_{\mathrm{Dij}} = \begin{bmatrix} 1/R_{\mathrm{dcij}} & -k/R_{\mathrm{dcij}} \\ -k/R_{\mathrm{dcij}} & k^2/R_{\mathrm{dcij}} \end{bmatrix} \tag{13}$$

2.4.3 DC load model: The DC load models can be divided into three types: constant resistance type, constant current type, and constant power type. It can also be a hybrid type of the three. The relationship between the load power P_{dcD} and the bus voltage U_{dc} is shown in formula (14).

$$P_{\mathrm{dcD}}(U_{\mathrm{dc}}) = A_R U_{\mathrm{dc}}^2 + A_C U_{\mathrm{dc}} + A_P \tag{14}$$

where A_R, A_C and A_P are the coefficients of constant resistance, constant current, and constant power model types, respectively.

2.5 DC distributed power and energy storage device model

There are some common DGs such as photovoltaic cells, wind turbine generators, fuel cells, and so on. The power generated by above DG sources is DC energy or can be converted to DC after a simple transformation. Furthermore, the energy storage devices like batteries and supercapacitors provide power and voltage supports for the distribution system, when needed, cooperating with a bidirectional DC/DC converter to deliver power to the grid, and to charge or disconnect to the grid when the system is in stability status. DGs and energy storage devices can be directly connected to the DC grid, so that many conversion steps can be omitted. Table 1 lists the steps for the above devices connecting to the grid. As is demonstrated in it, the integration of these devices into DC distribution network will save steps and costs.

According to different operating characteristics, distributed power sources can be handled as constant DC current model, constant DC power model and etc. since the charging or rather discharging condition can be controlled, energy storage devices are considered as constant power model. In power flow calculation, the active power of these DGs and energy storage equipment needs to be obtained in advance. Take the photovoltaic generation system as an example which is illustrated in Fig. 2. P_{mpp} is the maximum output power of photovoltaic cells under IEC standard conditions; T and I_{rr} are, respectively, the temperature and sunlight intensity surrounding the photovoltaic cells; F_T is the correction coefficient

used to describe the relationship between the actual output power and temperature; β_{PV} is the power loss factor of the DC/DC converter. (Fig. 4)

When the power flow is calculated, the $P_{PV,cell}$ can be approximated as a proportional relation to the light intensity, and the relationship with temperature can be expressed by F_T, as shown in (15).

$$P_{PV,cell} = \eta_d I_{rr} P_{mpp} F_T \tag{15}$$

with η_d characterising the loss of sunlight. The output power of photovoltaic cell is given by

$$P_{PV,con} = (1 - \beta_{PV}) P_{PV,cell} \tag{16}$$

As for wind power, its output power P_V mainly depends on the wind speed v at the height of the fan hub. The relationship between them can be expressed approximately by

$$P_V = \begin{cases} 0 & v < v_{ci}, v > v_{co} \\ P_r \dfrac{v - v_{ci}}{v_r - v_{ci}} & v \le v_{ci} < v_r \\ P_r & v_r \le v < v_{co} \end{cases} \tag{17}$$

where P_r is the fan's rated output power; v_r, $v_{ci,}$ and $v_{co,}$ respectively, indicate the fan's rated wind speed, cut-in wind speed, and cut-out wind speed.

2.6 DC grid power flow model

With regard to a DC distribution network with n buses, the relation among the DC current vector $\boldsymbol{I}_{dc}$, the DC voltage vector $\boldsymbol{U}_{dc}$ and the DC network bus admittance matrix $\boldsymbol{Y}_{dc}$ can be expressed as

$$\boldsymbol{I}_{dc} = \boldsymbol{Y}_{dc} \boldsymbol{U}_{dc} \tag{18}$$

where $\boldsymbol{I}_{dc} = [I_{dc1}, I_{dc2}, \ldots, I_{dcn}]^T$ is the bus current vector; $\boldsymbol{U}_{dc} = [U_{dc1}, U_{dc2}, \ldots, U_{dcn}]^T$ is the bus voltage vector; $\boldsymbol{Y}_{dc}$ is DC the bus admittance matrix.

The injection power at the DC bus i is given by

$$P_{dci} = P_{c,dci} + P_{Gi} - P_{dcDi} \tag{19}$$

where $P_{c,dci}$ is the active power transmitted by other DC lines or VSC converts to bus i; P_{Gi} is the active power of DGs or energy storage devices that input to bus i; P_{dcDi} is the power absorbed by DC loads, which is determined by (14). Moreover, the DC bus injection power P_{dci}, bus current I_{dci} and bus voltage U_{dci} have the following relationship

$$P_{dci} = I_{dci} U_{dci} \tag{20}$$

From (18)–(20), the DC bus injection power can be expressed as

$$P_{dci} = \sum_{j=1}^{n} Y_{ij} U_{dcj} U_{dci} \tag{21}$$

Thus, DC grid power flow calculation equation is given by

$$\Delta P_{dci} = P_{dcis} - \sum_{j=1}^{n} Y_{ij} U_{dcj} U_{dci} = 0 \quad i = 1, 2, \ldots, n \tag{22}$$

where ΔP_{dci} and P_{dcis} are the power mismatch and given active power of bus i, respectively.

3 AC&DC power flow calculation

3.1 VSC-MTDC control strategy

A VSC converter can independently control active power and reactive power through DQ decoupling method. Therefore, according to VSC different control, the system operating modes have a variety of combinations.

3.1.1 Master-slave control strategy: Master-slave control strategy is to select a converter as the main converter (generally the largest capacity converter), also called as voltage station. This converter station definitely adopts constant DC voltage control without any exception, control equation of which is shown as (23). The remaining converters are slave converters, using constant DC power control, also called as power stations, control equations of which is shown as (24). The voltage-power characteristics of the master-slave control strategy are shown in Fig. 5.

$$U_{dci} = U_{dcrefi} \tag{23}$$

$$P_{dci} = P_{dcrefi} \tag{24}$$

where U_{dcrefi} and P_{dcrefi} are, respectively, the reference values of DC-side voltage and active power of the converter.

The objective of the main converter is to maintain a constant DC voltage and to balance the active power in DC grid, which is considered as a slack bus in power flow calculation. There is ordinarily one slack bus in a DC grid. If there are any faults in the voltage station, one spare convertor will shift control mode from active power control to constant DC voltage control. The initial active power value from voltage station injected into AC system is given by

$$P_{dc1}^{(0)} = -\sum_{i=2}^{n} P_{dci}^{(0)} \tag{25}$$

where $P_{dci}^{(0)}$ is the initial active power value of other converter buses or DC buses; n is the total number of converters and DC buses.

As to power station, the AC-side control mode mainly includes the constant reactive power control and the constant AC voltage control. It has some similarities with the DGs, which are equivalent to virtual generator PV buses or PQ buses.

3.1.2 Droop control strategy: Droop control strategy mainly refers to the strategy that converters under the DC voltage-power droop control, shown in (26), are able to share loads with each other in order to ensure the stability of the DC voltage. The converter automatically adjusts its DC power according to measured DC voltage to satisfy power demand of the DC grid. The voltage-power characteristics of the droop control strategy are shown in Fig. 6.

$$f_i = P_{dci} - P_{dcrefi} + (U_{dci} - U_{dcrefi})/K_i = 0 \tag{26}$$

with K_i the converter droop coefficient, the larger K_i means that the converter affords smaller unbalanced power.

In power flow calculation, the initial active power value $P_{dci}^{(0)}$ of voltage-power droop convert i injected into AC system is taken as its reference value P_{dcrefi}.

3.2 Power flow calculation

Through the network topology analysis first, the whole system can be divided into several AC subsystems and DC subsystems. Furthermore, based on mathematical models of components in each subsystem, the node admittance matrix can be, respectively, formed, and thus the corresponding system equations are formulated in order to conduct power flow calculation.

3.2.1 AC system power flow: When calculating AC power flow, an AC bus connected to a VSC is regarded as a virtual generator bus. Depending on the control method, it can be equivalent to a PV

Table 2 Types and initial values of VSC buses

Control method	AC bus type	AC initial power	DC bus type	DC initial power
constant DC power	PQ	$P_i^{(0)} = P_{dcrefi}$ $Q_i^{(0)} = 0$	P	$U_{dci}^{(0)} = 1.0$
constant DC voltage	PV	$P_i^{(0)} = -P_{dc1}^{(0)}$ $U_i^{(0)} = 1.0$	slack	$P_{dc1}^{(0)} = -\sum_{i=2}^{n} P_{dci}^{(0)}$
droop control	PQ	$P_i^{(0)} = P_{dci}^{(0)}$ $Q_i^{(0)} = 0$	droop	$U_{dci}^{(0)} = U_{dcrefi}$ $P_{dci}^{(0)} = P_{dcrefi}$
constant reactive power	PQ	$U_i^{(0)} = 1.0$ $\delta_i^{(0)} = 0$	—	—
constant AC voltage	PV	$Q_i^{(0)} = 1.0$ $\delta_i^{(0)} = 0$	—	—

bus or a PQ bus. For starting each iteration, the initial values of virtual generator buses need to be given. Since the active power output of a converter depends on the DC-side power-balanced capacity, the reactive power output is independent of each other and depends on whether the converter controls the voltage or not. The DC-side control method of each converter determines the initial active power value while AC-side determines initial reactive power value. Table 2 shows the initial iterative power and different bus types of VSC converter stations.

The three-phase unbalanced AC power flow calculation is based on the forward/backward sweep method [11–13].

3.2.2 DC system power flow: During the DC power flow calculation, according to the control mode, the DC-side bus of a VSC converter is equivalent to P bus, slack bus, and droop bus. The VSC's DC-side bus types and initial power are similarly demonstrated in Table 2. Meanwhile, the DC bus with no DG or VSC connected is considered as a P bus and its power is given by (14). Eventually, the DC bus initial value is given by (19).

When adopting master-slave control strategy, it is assumed that the first DC bus is a slack bus which is connected to the main converter station and the remaining ones are *P* buses. Therefore, the system equations required to be solved for DC power flow calculation is

$$\boldsymbol{F}_{\mathrm{ms}}(\boldsymbol{X}_{\mathrm{ms}}) = [\Delta P_{\mathrm{dc1}} \quad \Delta P_{\mathrm{dc2}} \quad \dots \quad \Delta P_{\mathrm{dcn}}]^T = 0 \tag{27}$$

where the variables vector to be solved $\boldsymbol{X}_{\mathrm{ms}}$ is

$$\boldsymbol{X}_{\mathrm{ms}} = [P_{\mathrm{dc1}} \quad U_{\mathrm{dc2}} \quad U_{\mathrm{dc3}} \quad \dots \quad U_{\mathrm{dcn}}]^T \tag{28}$$

The above non-linear equations can be calculated with Newton–Raphson (NR) method, the mismatch vector $\Delta\boldsymbol{X}_{\mathrm{ms}}$ is given by

$$\boldsymbol{X}_{\mathrm{ms}} = \boldsymbol{J}_{\mathrm{dc}}^{-1}\boldsymbol{F}_{\mathrm{ms}}(\boldsymbol{X}_{\mathrm{ms}}) \tag{29}$$

with $\boldsymbol{J}_{\mathrm{dc}}^{-1}$ the inverse matrix of Jacobian matrix for non-linear equations.

As for droop control strategy, it is assumed that the former *m* buses are droop buses, which are connected to VSC stations and the rest are *P* buses linking no VSC. The variables vector to be solved $\boldsymbol{X}_{\mathrm{dr}}$ is

$$\boldsymbol{X}_{\mathrm{dr}} = [P_{\mathrm{dc1}} \quad \dots \quad P_{\mathrm{dcm}} \quad U_{\mathrm{dc1}} \quad U_{\mathrm{dc2}} \quad \dots \quad U_{\mathrm{dcn}}]^T \tag{30}$$

The above vector $\boldsymbol{X}_{\mathrm{dr}}$ contains unknown *m* buses' DC power and all *n* buses' DC voltage which is an $n+m$ dimensional vector, while (27) just provides only *n* formulas, so that other *m* equations is added it in order to satisfy NR solution conditions. Given that the

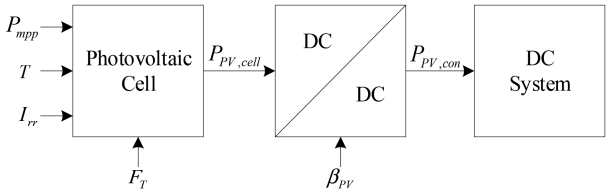

Fig. 4 *Structure of photovoltaic generation system*

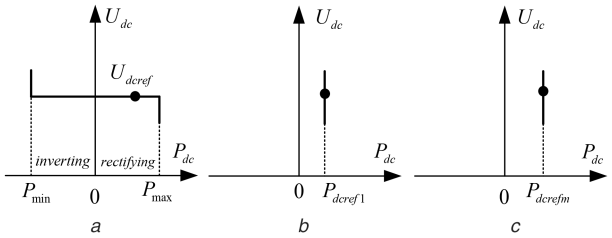

Fig. 5 *Master-slave control strategy*
(a) main converter, ***(b)*** slave convert *i*, ***(c)*** slave convert *m*

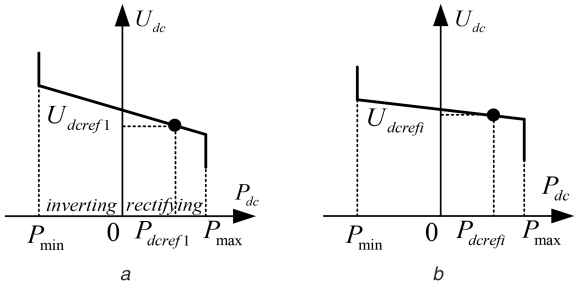

Fig. 6 *Droop control strategy*
(a) droop control convert 1, ***(b)*** droop control convert *i*

former *m* buses adopts droop control strategy, (26) is added to form new system equations as

$$\boldsymbol{F}_{\mathrm{dr}}(\boldsymbol{X}_{\mathrm{dr}}) = \begin{bmatrix} \boldsymbol{F}_{\mathrm{ms}}(\boldsymbol{X}_{\mathrm{dr}}) \\ \boldsymbol{F}(\boldsymbol{X}_{\mathrm{dr}}) \end{bmatrix}^T = 0 \tag{31}$$

with $\boldsymbol{F}(\boldsymbol{X}_{\mathrm{dr}}) = [f_1, f_2, \dots, f_m]^T$.

3.2.3 AC/DC sequential power flow iteration: The key of calculating sequential AC/DC power flow is to solve the coupling relationship between AC's and DC's power flow. First, the impact of AC system on DC system is generated by the converter bus voltage $U_s\angle\delta_s$. If this voltage is known, the DC system's power flow can be solved independently. Likewise, the effect of the DC system on the AC system is generated by the converter's AC power injection $S_s = P_s + jQ_s$. If this power is known, the AC system's power flow can also be solved independently. Therefore, AC voltage $U_s\angle\delta_s$ and active power injection P_s of a VSC converter is used as global iterative convergence variable. When the error of two calculations is less than the set value of toleration error ε, the sequential iteration algorithm converges and specific iteration process is depicted in Fig. 7.

4 Case study

As is illustrated in Fig. 8, a hybrid AC&DC distribution system is composed by adding DC grids into the IEEE 13 Node Test Feeder. IEEE 13 Node Test Feeder is three-phase unbalanced AC distribution network [14]. We renumber the buses of the AC and DC grids, respectively, in order to facilitate the description.

It is assumed that the 1, 2 and 12 AC buses are, respectively, connected with VSC converters, which form a circle DC distribution network with three-terminal VSC-MTDC and recorded as DC grid 1. Droop control strategy is applied to this DC grid whose voltage level is 4.16 kV. What's more, another typical radial DC distribution network links AC bus 3 through a VSC converter,

which adopts master-slave control strategy and recorded as DC grid 2. As there is only one VSC converter, no slave station is presented in this DC grid, thus, VSC 4 is selected as a slack bus and its voltage level is identically 4.16 kV. Then, through a DC/DC converter, voltage level changes to 1.5 kV. At AC bus 7 and 12, DGs of photovoltaic and wind integrate to AC side of grid. DC bus 12 is an island bus using constant voltage control. DC bus 5, 7, 10 and 11, respectively, connect different kinds of DGs. The base power is 100 MVA and the tolerance error ε is 1×10^{-6}.

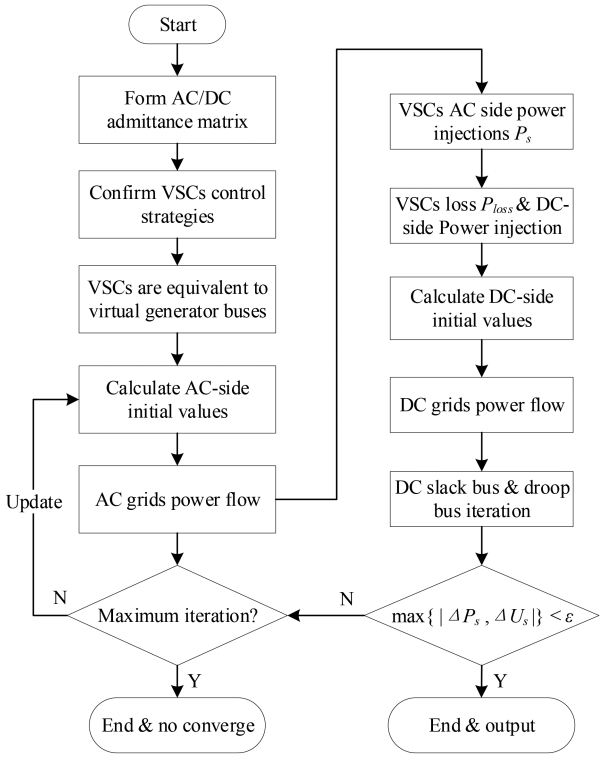

Fig. 7 *Sequential iterative process flow chart*

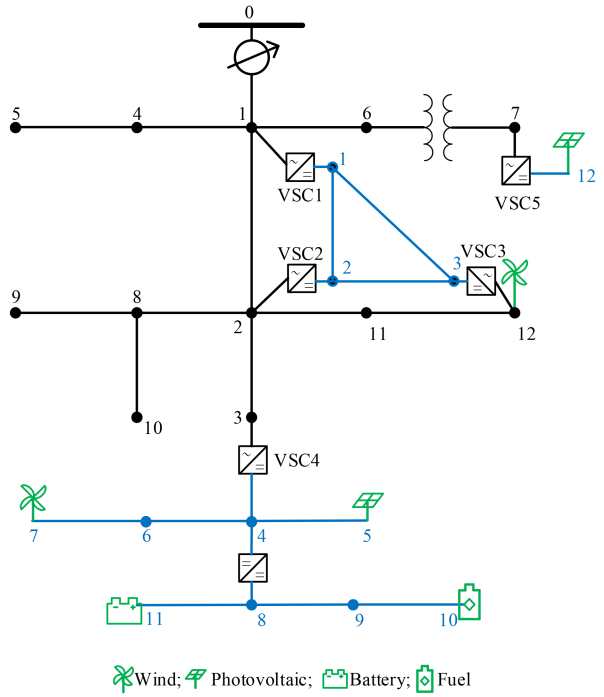

Fig. 8 *Modified IEEE 13 Node Test Feeder with VSC-MTDC*

The system includes DC loads (Table 3), DGs and energy storage devices (Table 4), VSC converters (Table 5), and many other DC devices.

Simulating the AC&DC system case in a personal computer with CPU Intel core i7 6700HQ @ 2.6 GHz and 8 GB RAM. Repeatedly employing the above AC/DC sequential iteration algorithm, each power flow calculation is converged by two iterations and in 0.13 s on average.

With DGs and DC network presented in the system, the calculating results of AC and DC grid voltages are shown in Tables 6 and 7. Convert stations' power loss is listed in Table 8. When the flexible DC structure is used to transmit renewable energy, the influence on the three-phase voltage of the entire AC system is demonstrated in Fig. 9.

Under different control strategies, the sequential iteration algorithm has excellent convergence and rapidity and the calculation results are accurate compared with [9, 10, 14]. Renewable energy which is connected to the grid through VSC-MTDC can flexibly regulate the system's power flow distribution. It is verified that the voltage distribution of AC system can be improved by adopting flexible DC distribution system, as shown in Fig. 9. The three-phase unbalanced level of AC voltage can be meliorated by further studying the compensation control of the VSC converters. The calculation algorithm described in the paper is still applicable.

In DC grid 1, voltage magnitudes of the bus 1, 2, and 3 serving as droop buses are 7.62, 7.5225, and 7.5075 kV (7.5 kV is 1.0 per-unit value). In DC grid 2, the bus 4 operates as a slack bus with a voltage magnitude of 7.5 kV (1.0 p.u.). The two distribution networks incorporate in a large number of DGs, making parts of the DC bus voltages are raised.

VSC's losses are exactly low, even the maximum power transaction of VSC 4, 215 kW loss is barely accounted for ~ 1% of total transmission power. It is also found that the hybrid power supply system can reduce the system lines' power loss from 157.33 to 120.07 kW compared with applying AC distribution network merely. It is manifested in above results that the proposed AC/DC sequential algorithm can account for unbalanced three-phase AC system and effectively handle a variety of control strategies. It can accurately and reliably analyse the system power loss and voltage level of the distribution network. In the same way, this method provides an effective analysis tool for power flow optimisation and operation management.

5 Conclusion

Here, an AC/DC sequential calculation algorithm suitable for unbalanced three-phase systems and AC&DC hybrid distribution networks is proposed by employing three-phase unbalanced models of AC grid, considering various kinds of DC models such as lines, loads, energy storage, and so on, analysing the VSC converter model and different operation control modes in detail. When calculating power flow, VSC converters in master-slave control strategy and droop control strategy are equivalent to different AC buses. Considering that three-phase unbalanced AC-side grid and

Table 3 Load data in DC Grid

DC Bus	Constant load type	Capacity/MW	DC bus	Constant load type	Capacity/MW
1	P	0.02	7	R	0.54
2	P	0.015	8	P	0.13
3	P	0.015	9	I	0.34
4	—	—	10	P	0.15
5	P	0.76	11	I	0.38
6	R	0.39	12	P	0

Table 4 DG configuration in distribution network

Grid	DG bus	Capacity/kVA	P_{mpp}/kW	P_f/kW	Real power/kW
DC grid	5	250	200		196
	7	150		150	100
	10	200	200		150
	11	200			100
	12	250		250	200
AC grid	12	200		200	150

Table 5 VSC parameter in distribution network

Equipment	*P* set/kW	*Q* set/kVA	*V* set/p.u.	Droop coefficient	$a, b, c/10^{-3}$
VSC1	2500	2500	1.008	0.005	15, 1.1, 2.5
VSC2	0	0	1	0.007	12, 1.3, 4.7
VSC3	1500	1500	0.994	0.005	13, 1.4, 3.5
VSC4	3000	—	1	—	11, 1.5, 1.4
VSC5	200	—	1	—	11, 1.5, 1.4

Table 6 Voltage of AC grid

AC bus	Phase A		Phase B		Phase C	
	Mag./p.u.	Ang./°	Mag./p.u.	Ang./°	Mag./p.u.	Ang./°
0	1.000	0.00	1.000	−120.00	1.000	120.00
1	1.021	−2.49	1.042	−121.72	1.017	117.83
2	0.969	−5.23	1.041	−122.54	0.959	116.05
3	0.961	−6.04	1.036	−123.28	0.951	115.17
4	—	—	1.033	−121.90	1.015	117.86
5	—	—	1.031	−121.97	1.013	117.90
6	1.018	−2.55	1.040	−121.76	1.014	117.82
7	0.994	−3.23	1.022	−122.22	0.996	117.35
8	0.968	−5.25	—	—	0.957	115.93
9	—	—	—	—	0.955	115.77
10	0.962	−5.18	—	—	—	—
11	0.970	−5.23	1.041	−122.54	0.959	116.05
12	0.966	−5.21	1.044	−122.52	0.960	116.35

Table 7 Voltage of DC grid

DC Bus	1	2	3	4	5	6
voltage/p.u.	1.016	1.003	1.001	1.000	0.997	0.997

DC Bus	7	8	9	10	11	12
voltage/p.u.	0.995	0.990	0.983	0.983	0.988	1.000

Table 8 VSC convert power loss

VSC	1	2	3	4	5
power loss/kW	30	4	10	215	2

diverse structures of DC grid exert a great influence on entire system and the control of converters, the method can converge rapidly. Through the calculation and analysis of the modified IEEE 13 Node Test Feeder incorporating renewable energy at DC-side grid, it is shown that the proposed method has good convergence and calculation accuracy for solving the three-phase unbalanced and complex VSC converter operation modes. Based on the research, the interaction between AC and DC sides of power system or rather the control method for compensation from VSC converts to AC-side unbalanced system can be further studied.

6 Acknowledgments

This work is supported by the Science and Technology Plan Projects of Colleges and Universities in Shandong Province (Project no. J17KA074).

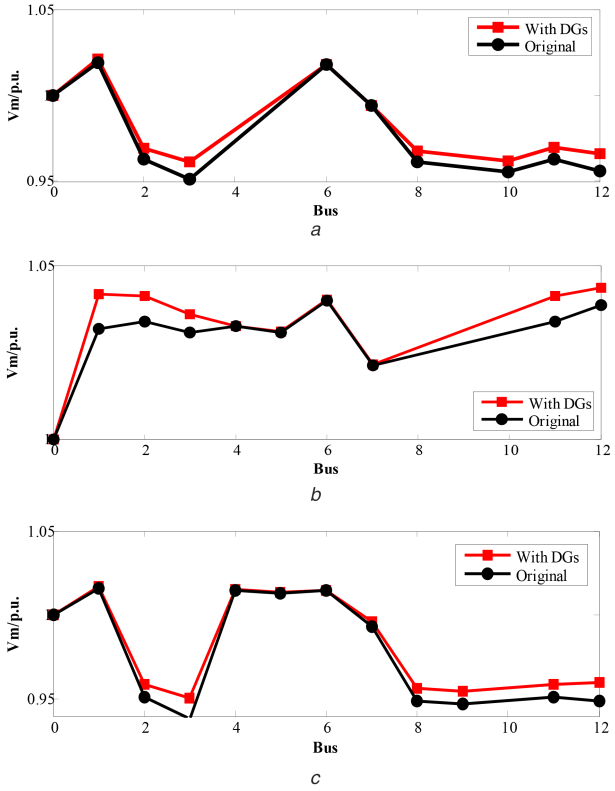

Fig. 9 *Impact of voltage distribution caused by DG*
(a) Phase A voltage magnitude, ***(b)*** Phase B voltage magnitude, ***(c)*** Phase C voltage magnitude

7 References

[1] Weichao, Z., Haifeng, L., Zhou, B., *et al.*: 'Review of DC technology in future smart distribution grid'. Proc. IEEE PES Conf. Innovative Smart Grid Technologies, Columbia, USA, January 2012, pp. 1–4

[2] Wang, P., Goel, L., Liu, X., *et al.*: 'Harmonizing AC and DC: A hybrid AC/DC future grid solution', *IEEE Power Energy Mag.*, 2013, **11**, (3), pp. 76–83

[3] Gengyin, L., Ming, Z., Jie, H., *et al.*: 'Power flow calculation of power systems incorporating VSC-HVDC'. Proc. IEEE PowerCon, Singapore, November 2004, vol. 2, pp. 1562–1566

[4] Gonzalez-Longatt, F., Roldan, J.M., Charalambous, C.A.: 'Solution of AC/DC power flow on a multiterminal HVDC system: illustrative case supergrid phase I'. Proc. 47th Int. Universities Power Eng. Conf., London, UK, September 2012, pp. 1–7

[5] Beerten, J., Cole, S., Belmans, R.: 'Generalized steady-state VSC MTDC model for sequential AC/DC power flow algorithms', *IEEE Trans. Power Syst.*, 2012, **27**, (2), pp. 821–829

[6] Beerten, J., Van Hertem, D., Belmans, R.: 'VSC MTDC systems with a distributed DC voltage control – A power flow approach'. Proc. IEEE PowerTech., Trondheim, Norway, June 2011, pp. 1–6

[7] Sameni, A., Nassif, A.B., Opathella, C., *et al.*: 'A modified Newton-Raphson method for unbalanced distribution systems'. Proc. IEEE Int. Conf. Smart Grid Engineering, Oshawa, Canada, August 2012, pp. 1–7

[8] Kersting, W.H.: '*Distribution system modeling and analysis*' (CRC Press, Boca Raton, 2002, 3rd edn. 2012)

[9] Daelemans, G.: 'VSC HVDC in meshed networks'. Master's thesis, Katholieke Universiteit Leuven, 2008

[10] Cole, S.: 'Steady-state and dynamic modeling of VSC HVDC systems for power system simulation'. PhD thesis, Katholieke Universiteit Leuven, 2010

[11] Samal, P., Ganguly, S.: 'A modified forward backward sweep load flow algorithm for unbalanced radial distribution systems'. Proc. IEEE Int. Conf. Power & Energy Soc. Gen. Meet., Colorado, USA, July 2015, pp. 1–5

[12] Khushalani, S., Solanki, J.M., Schulz, N.N.: 'Development of three-phase unbalanced power flow using PV and PQ models for distributed generation and study of the impact of DG models', *IEEE Trans. Power Syst.*, 2007, **22**, (3), pp. 1019–1025

[13] Yuntao, J., Wenchuan, W., Boming, Z., *et al.*: 'An extension of FBS three-phase power flow for handling PV nodes in active distribution networks', *IEEE Trans. Smart Grid.*, 2014, **5**, (4), pp. 1547–1555

[14] 'IEEE 13 Node Test Feeder'. Available at http://www.ewh.ieee.org/soc/pes/dsacom/testfeeders/feeder13.zip, accessed 5 January 2018